iScience

CellPress
OPEN ACCESS

Article

Bactericidal, anti-biofilm, and anti-virulence activity of vitamin C against carbapenem-resistant hypervirulent *Klebsiella pneumoniae*

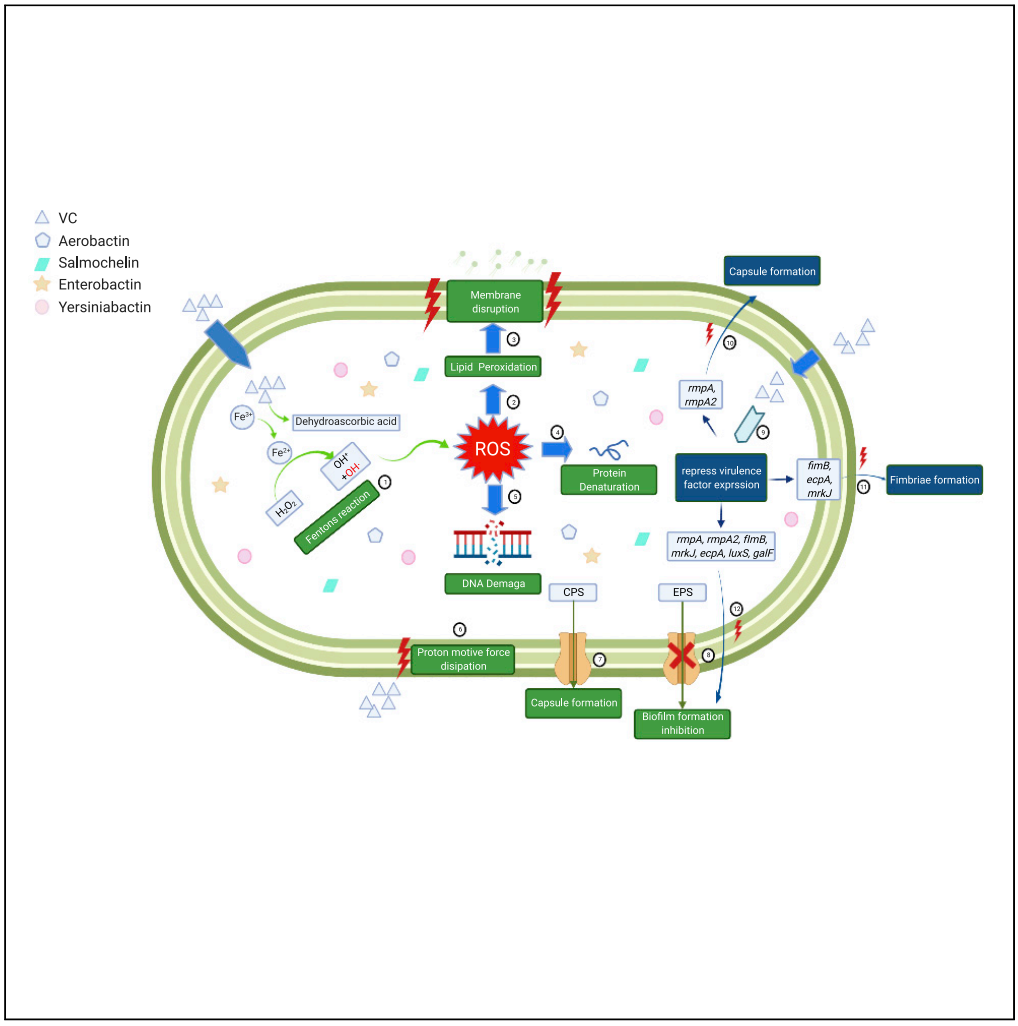

Chen Xu, Ning Dong, Kaichao Chen, ..., Edward Wai Chi Chan, Xi Yao, Sheng Chen

shechen@cityu.edu.hk

Highlights

VC exhibited bactericidal and anti-biofilm effects on CR-hvKP

The bactericidal effect of VC is associated with induction of ROS production

VC acted as an efflux pump inhibitor to disrupt transportation of EPS and CPS

VC could suppress the expression of virulence-associated genes in CR-hvKP

Xu et al., iScience *25*, 103894
March 18, 2022
https://doi.org/10.1016/j.isci.2022.103894

iScience

CellPress
OPEN ACCESS

Article

Bactericidal, anti-biofilm, and anti-virulence activity of vitamin C against carbapenem-resistant hypervirulent *Klebsiella pneumoniae*

Chen Xu,[1] Ning Dong,[1] Kaichao Chen,[1] Xuemei Yang,[1] Ping Zeng,[2] Changshun Hou,[3] Edward Wai Chi Chan,[2] Xi Yao,[3] and Sheng Chen[1,4,*]

SUMMARY

The emergence of carbapenem-resistant hypervirulent *Klebsiella pneumoniae* (CR-hvKP) causing high mortality in clinical patients infers the urgent need for developing therapeutic agents. Here, we demonstrated vitamin C (VC) exhibited strong bactericidal, anti-biofilm, and virulence-suppressing effects on CR-hvKP. Our results showed such a bactericidal effect is dose-dependent both *in vitro* and in the mouse infection model and is associated with induction of reactive oxygen species (ROS) generation. In addition, VC inhibited biofilm forma tion of CR-hvKP through suppressing the production of exopolysaccharide (EPS). In addition, VC acted as an efflux pump inhibitor at subminimum inhibitory concentration (sub-MIC) to disrupt transportation of EPS and capsular polysaccharide to bacterial cell surface, thereby further inhibiting biofilm and capsule formation. Furthermore, virulence-associated genes in CR-hvKP exposed to sub-MIC of VC were downregulated. Our findings indicated VC could be an effective and safe therapeutic agent to treat CR-hvKP infections in urgent cases when all current treatment options fail.

INTRODUCTION

Klebsiella pneumoniae is a notorious opportunistic pathogen which often causes multi-organ infections such as pneumonia, urinary tract infections, bacteremia, and liver abscesses (Paczosa and Mecsas, 2016). In the mid-1980s, hypervirulent *K. pneumoniae* (hvKP) that caused liver abscesses was first reported in Taiwan (Shon et al., 2013). The hvKP strain is significantly more virulent than the classic *K. pneumoniae* (cKp) strain because it could cause invasive and metastatic infections even in young, healthy individuals (Sellick and Russo, 2018). This variant of *K. pneumoniae* is now undergoing global dissemination and cases are being reported from Asia (Gu et al., 2018; Chen and Chen, 2021), Europe(Decré et al., 2011), the United States (Karlsson et al., 2019), Australia (Turton et al., 2007), and South Africa (Victor et al., 2007). Community-acquired infections because of hvKP are now regarded as a serious global threat, with rapid increase in incidence of infection cases (Namikawa et al., 2019). Antibiotic resistant cKP strains are also globally disseminated (Lee et al., 2016), but hvKP was reported to be rarely resistant to commonly used antibiotics, despite being intrinsically resistant to ampicillin (Lee et al., 2017). Previous studies showed that hypervirulent and antimicrobial-resistant populations of *K. pneumoniae* were largely nonoverlapping, yet a recent study reported the emergence of *K. pneumoniae* isolated with convergent hypervirulence and multidrug resistance (Zhang et al., 2016b). Most importantly, carbapenem-resistant hvKP (CR-hvKP) has emerged and caused fatal infections in hospital patients worldwide(Zhang et al., 2016a; Gu et al., 2018; Kalpoe et al., 2012; Borer et al., 2011). The convergence of phenotypic drug resistance and hypervirulence represents an even more serious threat to human health, because infections caused by multidrug resistant hvKP have limited treatment options, especially those involving carbapenem resistant hvKP (CR-hvKP), for which no effective therapeutic agents are available (Choby et al., 2020; Furlan et al., 2020; Lee et al., 2018).

Biofilm formed by HvKP strains may enhance the invasiveness of infection by allowing the organisms to colonize in gastrointestinal, respiratory, and urinary tracts (Piperaki et al., 2017). Biofilm also protects bacterial cells from immune defenses and antibiotics, resulting in the high-level resistance of hvKP to antimicrobial agents (Mah and O'toole, 2001). During the process of biofilm formation, exopolysaccharides (EPS) are produced and exported by bacterial cells, forming a matrix that protects the cells inside against the

[1]Department of Infectious Diseases and Public Health, Jockey Club College of Veterinary Medicine and Life Sciences, City University of Hong Kong, Kowloon, Hong Kong

[2]State Key Lab of Chemical Biology and Drug Discovery, Department of Applied Biology and Chemical Technology, The Hong Kong Polytechnic University, Hung Hom, Kowloon, Hong Kong

[3]Department of Biomedical Sciences, City University of Hong Kong, Kowloon, Hong Kong

[4]Lead contact

*Correspondence: shechen@cityu.edu.hk

https://doi.org/10.1016/j.isci.2022.103894

hostile environment and exposure to bioactive materials (Jung et al., 2013). Export of EPS across the inner membrane and subsequent translocation to cell surface are mainly mediated by efflux pumps (Schmid et al., 2015), inferring that inhibiting efflux activities may effectively disrupt biofilm formation of hvKP (Reza et al., 2019). On the other hand, the distinct virulence factors of hvKP include the siderophore systems which are functionally important for iron acquisition, capsule of the K1 and K2 capsular types, and the colibactin toxin (Choby et al., 2020). Among them, the capsule, which is comprised of high-molecular weight polysaccharide (CPS) and firmly attached to the bacterial cell surface, is the most studied virulence factor as it confers protection against the host immune response by inhibiting elicitation of early inflammatory signals (Paczosa and Mecsas, 2016). Hence, CPS has been considered a key target in development of therapeutics strategies and vaccine against hvKP (Opoku-Temeng et al., 2019).

Failure of existing antibiotics to eradicate CR-hvKP or attenuate its virulence level resulted in exhaustion of the last resort antibiotics (Zhao et al., 2019). There is an urgent need for therapeutic agents, especially those which are safe to mammalian cells and exhibit low tendency to select for resistant strains (Ling et al., 2015). Vitamin C (VC), also called ascorbic acid, is an essential nutrient of humans. VC is a potential antioxidant and known to be effective in treatment of scurvy, cardiovascular diseases, cancer, gout, and cataracts (Hodges et al., 1969; Vilchèze et al., 2013; Padayatty et al., 2003). Apart from the fact that VC plays an important role in human health, it has little side effects and is easily available at low cost Previous studies showed that VC exhibited high efficacy in killing Gram-positive strains by inducing oxidative stress, as well as the ability to inhibit biofilm formation in *Escherichia coli* (Vilchèze et al., 2013; Shivaprasad et al., 2021). In this work, we provide evidence to prove that VC can be used effectively to treat infections caused by CR-hvKP.

RESULTS AND DISCUSSION

High doses of VC eradicate CR-hvKP

In vitro susceptibility test results showed VC that exhibited antimicrobial effect on CR-hvKP strains KP1088 and HvKP3 with minimum inhibitory concentrations of 8 mg/mL and 16 mg/mL, respectively. The pH of LB broth with 8 mg/mL and 16 mg/mL VC were 4.08 and 3.85, respectively. We adjusted the pH of the medium from 4.0 to 7.0 and found that the acidic environment would not inhibit the growth of bacteria, indicating that the acidic environment itself would not have antibacterial activity. We also determined the MIC of KP1088 and HvKP3 treated with sodium acetate in MHB broth with different pH (4.0, 5.0, 6.0, and 7.0) and the MIC values were all 128 mg/mL, suggesting that acetate had weaker antibacterial effect than acetic acid and the acidic environment could not enhance the antibacterial effect of acetate.

To further elucidate the bactericidal effect of VC on the two CR-hvKP strains, a time-kill curve assay was performed. The growth of KP1088 at both early (Figure 1A) and late exponential phases (Figure 1B) were found to be inhibited by VC at 8 mg/mL (MIC) within 12 h. Bacterial cells in the late exponential phase were less sensitive than those in the early growth phase because VC at 2-fold MIC was required to eradicate the strains within 24 h. Similarly, VC at 16 mg/mL also exhibited a bactericidal effect on HvKP3 at both early exponential phase (Figure 1C) and late exponential phase (Figure 1D) upon incubation for 24-h at 37°C.

The potential of CR-hvKP to evolve into phenotypically VC resistant strains *in vitro* was determined by performing serial passages of KP1088 and HvKP3 under different concentrations of VC for a period of seven days or more. No resistant mutants emerged upon exposure to VC during the test period, indicating that CR-hvKP could not develop resistance to VC without losing physiological fitness (Figure 1E)

VC disrupts biofilm formation in CR-hvKP

Because biofilm plays a major role in expression of the resistance and virulence phenotypes of CR-hvKP, the ability of *K. pneumoniae* strain KP1088 and HvKP3 to form biofilm was evaluated by crystal violet assay. The cut-off value (OD_C) was found to be 0.12 and the final absorbance of *K. pneumoniae* strain KP1088 and HvKP3 biofilm were 0.2716 $\pm$ 0.0166 and 0.2503 $\pm$ 0.0028, respectively (Figure 2). As such, the two test strains (OD_{test}) were regarded as both moderate biofilm producers ($2*OD_C<OD_{test} \leq 4*OD_C$) after incubation for 24-h (Extremina et al., 2011). Compared to the biofilm biomass of *K. pneumoniae* KP1088 and HvKP3 which received no treatment, formation of *K. pneumoniae* KP1088 biofilm was found to be stimulated by 4 mg/mL of VC, yet 8 mg/mL of VC or a higher dosage inhibited biofilm formation in a dose-dependent manner (Figure 2A). On the other hand, 4 mg/mL of VC was sufficient to exhibit anti-biofilm effect on *K. pneumoniae* strain HvKP3, with further reduction of the HvKP3 biofilm biomass observable when treated

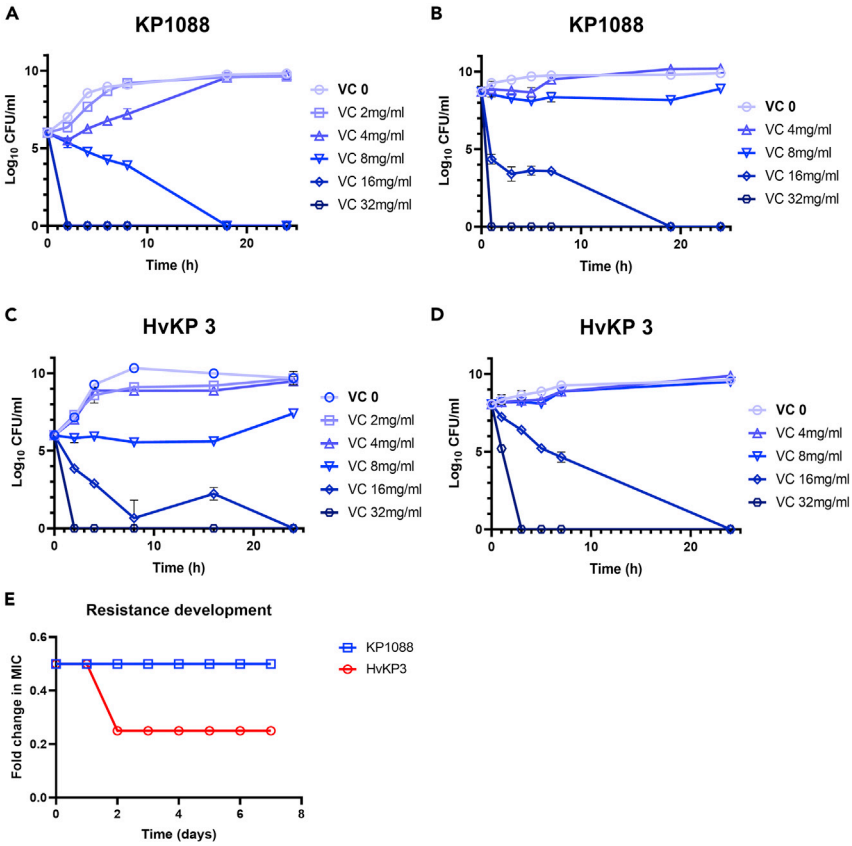

Figure 1. Time-kill curve and development of resistance of CR-hvKP strains KP1088 and HvKP3 treated with VC

(A) KP1088 in the early exponential phase treated with VC.

(B) KP1088 in the early exponential phase treated with VC.

(C) HvKP3 in the early exponential phase treated with VC.

(D) KP1088 in the late exponential phase treated with VC. The bacterial CFUs per mL at different time points during 24 h were determined. All experiments were performed in triplicate, and the mean ± SD is shown.

(E) Development of resistance to VC in KP1088 and HvKP3. Strain KP1088 and HvKP3 were subjected to serial passages in the presence of different concentrations of VC. The y axis is the highest concentration of VC the cells could grow during the serial passages. KP1088 could only grow in VC at 0.5*MIC and the highest concentration HvKP3 could grow was 0.25*MIC after incubation for three days

with higher doses of VC (Figure 2B). After biofilms of KP1088 and HvKP3 were treated with different concentrations of VC for 24 h, the viable cells were counted and recorded (Figures 2C and 2D). VC at 4 and 8 mg/mL could not inhibit the growth of both KP1088 and HvKP3, suggesting that the inhibition effect of 8 mg/mL of VC on biofilm was not coming from its antimicrobial effect. When biofilms of KP1088 and HvKP3 were treated with 16 mg/mL VC, a significant decrease in the number of viable cells ($p < 0.005$) was detected. Biofilm and EPS of the two strains treated with 16 mg/mL VC were also reduced, indicating that both the antimicrobial effect and the inhibition in EPS formation of VC resulted in the anti-biofilm activity of VC.

CLSM images suggested that VC can effectively inhibit biofilm formation in strains KP1088 and HvKP3 and disrupt existing biofilm on glass slides (Figure 2E). The cultures grown with VC at 8 mg/mL and 16 mg/mL or without VC followed by fixation and fluorescence staining with SYTOX Green (nucleic acid staining) were visualized using a confocal laser scanning microscope. The biofilm structure of the two cultures treated with VC appeared fragmented and fewer microcolonies were left on the slides after treatment. Biovolume of KP1088 and HvKP3 cells incubated with different concentrations of VC was also analyzed and calculated using COMSTAT (Technical University of Denmark, Lyngby, Denmark) (Figures 2F and 2G) (Heydorn et al., 2000; Vorregaard, 2008). Upon treatment with various concentrations of VC, biovolumes from biofilm of KP1088 and HvKP3 were significantly reduced in a dose-dependent manner.

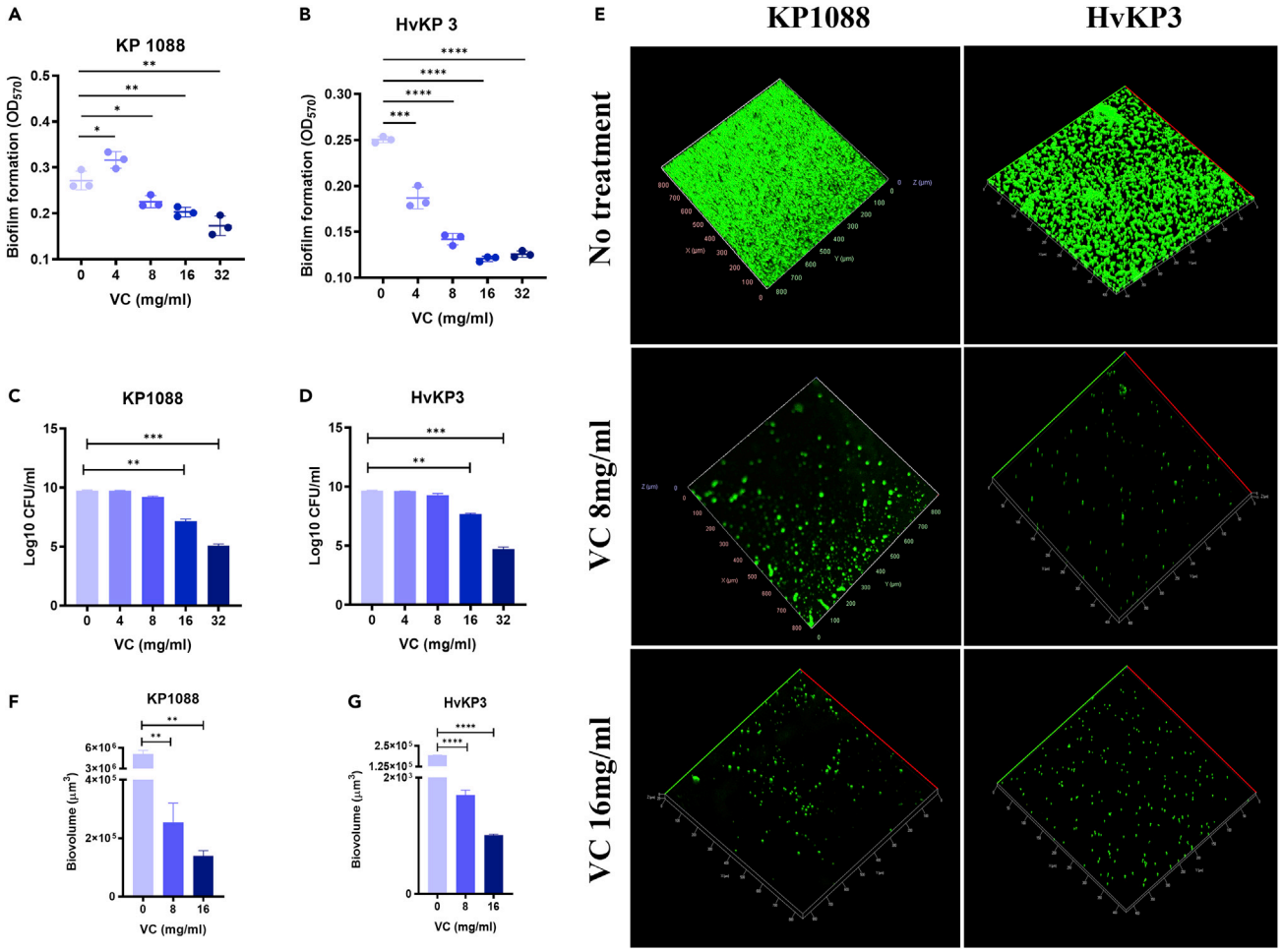

Figure 2. Biofilm formation in CR-hvKP strains upon treatment with VC

(A and B) Biofilm formation in KP1088 (A) and HvKP3 (B) upon treatment with different concentrations of VC for 24 h. Data are representative of their experiments performed in triplicate.

(C and D) Viable cell counting of KP1088 (C) and HvKP3 (D) biofilm treated with various concentrations of VC for 24 h.

(E) CLSM imaging of biofilm formation in strain KP1088 and HvKP3 upon treatment with VC. The left column is images of biofilm of KP1088 without treatment and after treatment with 8 mg/mL and 16 mg/mL of VC. The right column is images of HvKP3 biofilm without treatment and after treatment with 8 mg/mL and 16 mg/mL of VC.

(F) COMSTAT analysis of biovolumes from KP1088 biofilm treated with VC.

(G) COMSTAT analysis of biovolumes from HvKP3 biofilm treated with VC. *, $p < 0.05$, **, $p < 0.005$, ***$p < 0.0005$, ****$p < 0.00005$ (independent *t*-test).

To further ascertain that the changes in biofilm structure of the two strains was inflicted by VC, SEM imaging was performed to visualize the effect of low concentration VC (4 mg/mL, one-fourth MIC) on the biofilm of *K. pneumoniae* strain HvKP3. The biofilm of this strain formed well on glass slides but began to disintegrate upon treatment with even low concentration of VC (Figure 3).

Antimicrobial and anti-virulence effect of VC on CR-hvKP

Generation of ROS

The antimicrobial activity of VC was based on its prooxidant action and subsequent generation of ROS (Shivaprasad et al., 2021). Previous studies showed that high concentration of VC stimulated the generation of ROS in *Mycobacterium tuberculosis* cells, resulting in lipid oxidation, redox unbalance, and DNA damages (Vilchèze et al., 2013). Furthermore, ROS was also generated in *E. coli* during treatment with high concentration of VC, inhibiting bacterial growth (Shivaprasad et al., 2021). To evaluate the role of VC in inducing ROS production in CR-hvKP, DCF-DA assay was performed to measure cellular ROS accumulation because the DCF-DA fluorescence intensity is proportional to the ROS level. The fluorescence intensity of *K. pneumoniae* strain KP1088 and HvKP3

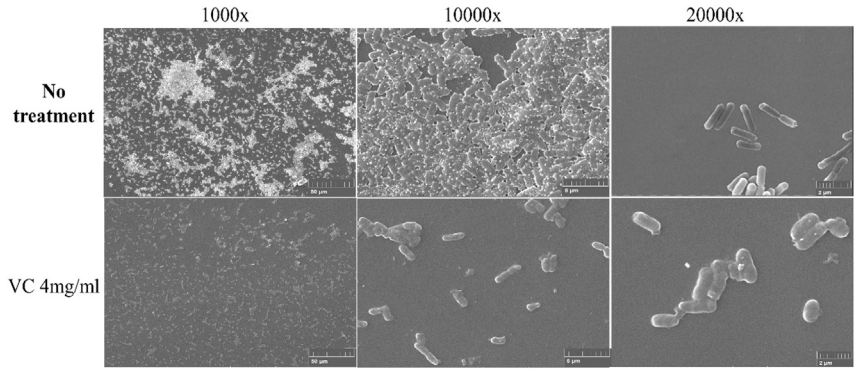

Figure 3. Scanning electron microscopic (SEM) images of HvKP3 biofilm

The upper panel is SEM images of HvKP3 biofilm without treatment and visualized by 1000-fold (left) 10,000-fold (middle) and 20,000-fold (right) magnification. The lower panel is SEM images of HvKP3 biofilm grown in the presence of 4 mg/mL of VC and visualized by 1000-fold (left),10,000-fold (middle) and 20,000-fold (right) magnification

treated with 8 mg/mL or 16 mg/mL of VC was found to increase when compared to the untreated control and an even higher rate of increase was observed when the VC concentration increased from 8 mg/mL to 16 mg/mL. These findings suggested that treatment with VC caused intracellular accumulation of ROS in *K. pneumoniae* strain KP1088 and HvKP3 in a dose-dependent manner (Figure 4A).

EPS production

Bacterial cell surface polysaccharide plays an important functional role in biofilm formation and virulence expression (Knecht et al., 2020). The organized type of polysaccharides was termed a capsule with a distinct structure (CPS), whereas the released type is an EPS (Majkowska-Skrobek et al., 2016). EPS is an essential component of the extracellular biofilm matrix in the biofilm scaffold (Ostapska et al., 2018). The function of EPS also includes protecting bacterial cells from antibiotics, environmental stress such as dehydration, and host immune defenses (Vu et al., 2009). As shown in Figure 4B, the production of EPS by *K. pneumoniae* strain KP1088 and HvKP3 treated with sub-MIC concentration of VC (2 mg/mL) was enhanced, yet higher concentration of VC was found to inhibit EPS production, as the amount of EPS produced by strain KP1088 and HvKP3 treated with 8 mg/mL VC was reduced by 3-fold and 5-fold, respectively.

CPS production

The virulence level of capsulated pathogenic bacteria is highly dependent on the structure of CPS (Cescutti, 2010). Uronic acid, which is an essential component in a capsule, has been used as a marker for quantification of the amount of capsular substance produced by bacterial pathogens (Walker et al., 2019). Figure 4C showed that VC could effectively reduce the CPS content in both test strains. Exposure of *K. pneumoniae* strain KP1088 to 4 mg/mL of VC leads to a 3-fold reduction in CPS production and VC-treated HvKP3 (4 mg/mL) exhibited a 10-fold reduction when compared to the untreated control.

Bacterial membrane proton motive force (PMF) dissipation

Because VC can serve as a stable donor of a single hydrogen atom which may undergo direct or concerted electron/proton transfer (Njus et al., 2020), we speculated that VC might cause bacterial PMF dissipation. A potential-sensitive dye, $DiSC_3(5)$, was employed to determine the effect of VC on CR-hvKP bacterial cell membrane PMF (Te Winkel et al., 2016). $DiSC_3(5)$ accumulates in polarized cells and would be released to media upon dissipation of bacterial membrane potential, resulting in increased fluorescence (Morin et al., 2011). Valinomycin, a K^+ carrier, was employed as the positive control. In comparison with the untreated cells, 5 μg/mL of valinomycin caused dissipation of the membrane potential of KP1088 and HvKP3 by increasing the membrane permeability to K^+ in a medium containing 100mM of KCl. Upon addition of VC, the membrane potential of KP1088 and HvKP3 was also found to dissipate rapidly, resulting in significant increase in fluorescence signal (Figure 5).

Efflux inhibition

Because most efflux transporters are driven by proton motive force, Nile red efflux assay was employed to examine the effect of VC on efflux pump activities (Li et al., 2015). Nile red is an efflux pump substrate which

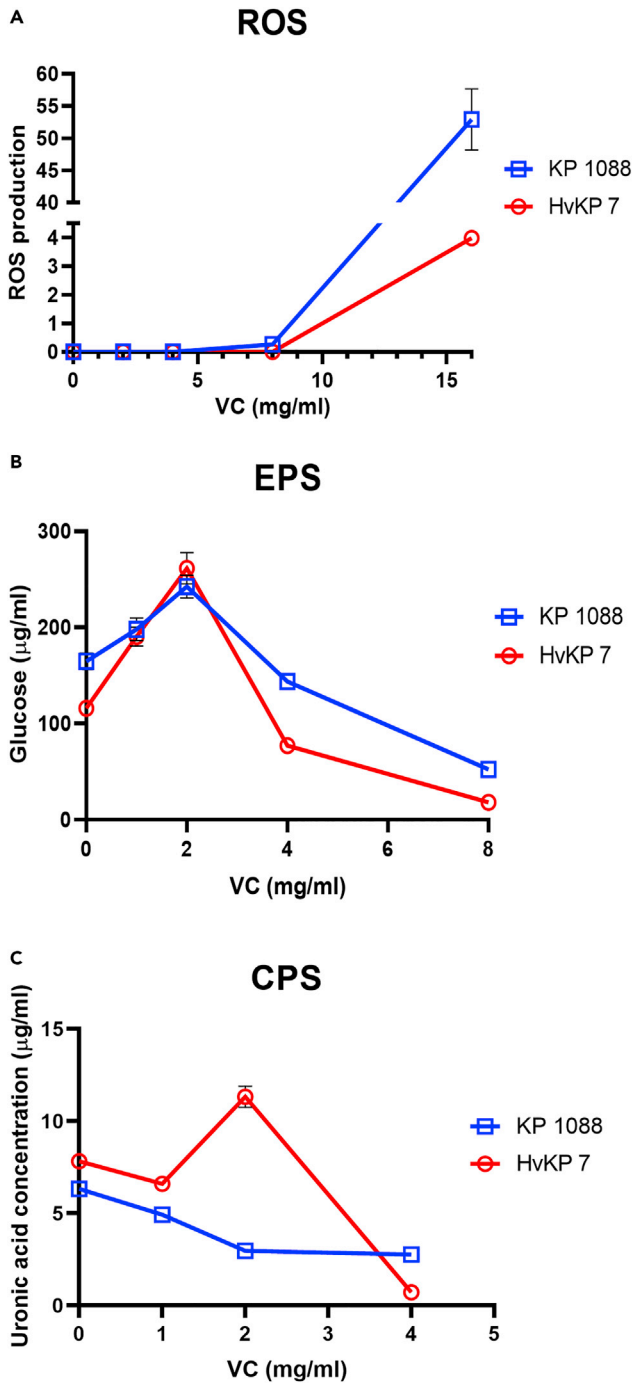

Figure 4. Antibacterial and anti-virulence effect of VC on *K. pneumoniae* strain KP1088 and HvKP3

(A) ROS generation in *K. pneumoniae* strain KP1088 and HvKP3 after 4 h exposure to VC of different concentrations. ROS production is expressed as the fluorescence intensity of ROS upon normalization to viable-cell counts. Anti-virulence effect of VC on *K. pneumoniae* strain KP1088 and HvKP3.

(B) EPS production in *K. pneumoniae* KP1088 and HvKP3 upon incubation overnight in the presence of different concentrations of VC. The production of EPS was determined and expressed as glucose equivalents by matching against a glucose standard curve.

(C) CPS production of KP1088 and HvKP3 incubated overnight in the presence of different concentrations of VC. CPS production was determined by matching against a uronic acid standard curve and normalized to the total viable bacterial cell counts. Results were expressed as uronic acid equivalents per 10^6 CFU. All experiments were performed in triplicate, and the mean ± SD is shown

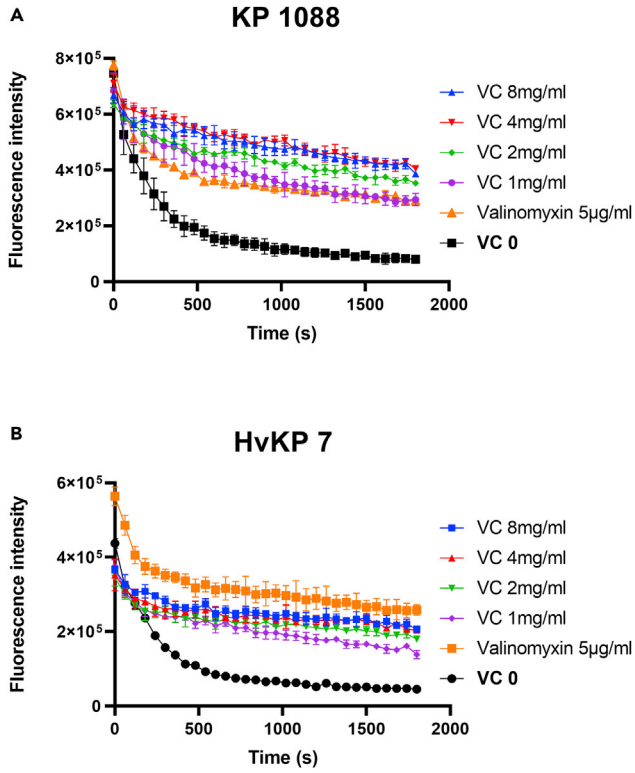

Figure 5. Membrane potential determination in CR-hvKP

(A and B) Determination of effect of different concentrations of VC on bacterial cell membrane potential of strain KP1088 (A) and HvKP3 (B). The K^+ transporter valinomycin (5μM) was used as positive control. The assay was conducted with 100mM of KCl. All experiments were performed in triplicate, and the mean ± SD is shown

becomes strongly fluorescent upon partitioning into the bacterial membrane and could be pumped out of the cell immediately (Bohnert et al., 2010). Carbonyl cyanide *m*-chlorophenylhydrazone (CCCP), an ionophore, was employed as a positive control to inhibit efflux activities (Baron and Rolain, 2018). Incubation of KP1088 (Figure 6A) and HvKP3 (Figure 6C) with VC resulted in reduction in export of Nile red in a dose-dependent manner. 50mM of glucose was then added to the test medium to test the ability to energize the efflux pump and restore efflux activities. The inhibitory effect of CCCP was effectively counteracted by addition of glucose and Nile red was rapidly transported out from bacterial cell membrane in the presence of glucose. In comparison, the energization effect of glucose was not obvious in cells treated with VC. Nevertheless, KP1088 and HvKP3 treated with 4 mg/mL of VC were still viable according to the time-kill curve, suggesting that the increase in fluorescence was not because of the death of the bacterial cell. Washout of CCCP eliminated the inhibition effect of Nile red efflux, yet washout of VC had no effect on the reduced Nile red efflux in KP1088 and HvKP3, confirming that the inhibitory effect of VC was not readily reversible by addition of glucose (Figures 6B and 6D) (Reens et al., 2018).

VC-induced alteration in gene expression

To further evaluate the anti-virulence activity of VC, the transcriptional responses of both strains KP1088 and hvKP3 in the presence of VC at 4 mg/mL were determined. The *rmpA* and *rmpA2* gene encode capsule biosynthesis and hence the mucoid phenotype in hvKP strains (Lin et al., 2019). According to previous studies, strain KP1088 carried both the *rmpA* and *rmpA2* genes, and that strain hvKP3 carried the *rmpA2* gene only (Gu et al., 2018; Zhang et al., 2016a). qRT-PCR analysis suggested that exposure to VC suppressed the expression of *rmpA2* in strain hvKP3 by 27.3-folds. In strain KP1088, expression of *rmpA* was suppressed by 2.8-folds by VC; however, *rmpA2* expression was not affected, with expression level being 1.5-fold of the non-treatment control (Figure 7). Based on these findings, we speculate that the anti-virulence activity of VC was associated with its ability to inhibit the transcription of capsule synthesis genes.

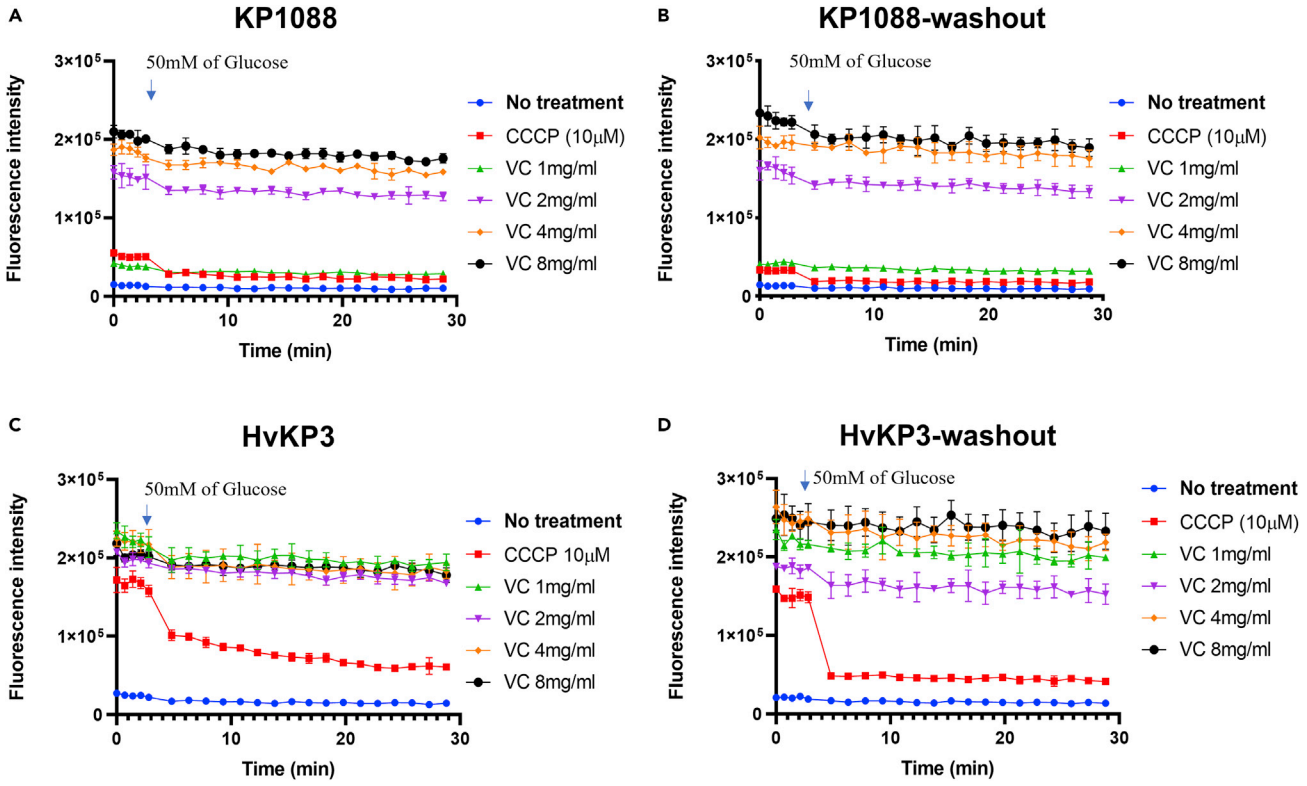

Figure 6. Inhibition of Nile Red efflux by VC in a dose-dependent manner

(A–D) Intensity of Nile Red fluorescence in strain KP1088 after treatment with different concentrations of VC; (B) Nile red fluorescence intensity of KP1088 after treatment of VC, followed by washout of VC after staining; (C) Nile red fluorescence of HvKP3 treated with different concentrations of VC; (D) Nile red fluorescence of HvKP3 upon treatment of VC and washout of VC after staining. 50 mM of Glucose was added to the assay at 2.8 min; the fluorescence was monitored for another 20 min. All experiments were performed in triplicate, and the mean ± SD is shown

Fimbriae are another major virulence factor of *K. pneumoniae* which plays a role in adherence of the bacterium to eukaryotic epithelial cells (Paczosa and Mecsas, 2016). The mannose-sensitive type 1 fimbriae encoded by the *fimABCDEFGHIK* locus and the mannose-resistant type 3 fimbriae encoded by the *mrkABCDFHJ* locus are major adhesive fimbriae structures (Paczosa and Mecsas, 2016). *K. pneumoniae* also produces a fimbria known as *E. coli* common pilus (ECP), with the *ecpA* gene encoding the major pilin subunit (Alcántar-Curiel et al., 2013). In this work, the *fimB*, *mrkJ*, and *ecpA* genes were found to be downregulated by 2.0, 6.2, and 5.3-folds in strain hvKP3 upon treatment with VC. In strain KP1088, the expression level of *ecpA* was suppressed by 20.0-folds after exposure to VC, but that of genes *fimB* and *mrkJ* did not alter significantly (Figure 7). The possibility that the anti-virulence activity of VC may be mediated through repressing the expression of fimbriae-associated genes cannot be ruled out.

To further confirm the inhibitory effect of VC on biofilm formation, the transcript levels of biofilm-associated genes of *luxS* and *galF* were tested, with results showing that there was a decrease in transcription of both genes in strain KP1088 (4.1 and 4.4-folds, respectively) upon exposure to VC. In strain hvKP3, the expression level of both genes was also slightly upregulated (by 2.5 and 1.1-folds, respectively). Previous studies demonstrated that external bacterial structures including fimbriae and capsules play an important role in biofilm formation (Ribeiro et al., 2016). The general trend of downregulation in expression of the biofilm-associated, capsule-associated, and fimbriae-associated genes is likely the molecular mechanism that underlies the anti-biofilm effect of VC on CR-hvKP strains.

VC exhibits antimicrobial effect in mouse infection model

The *in vivo* antimicrobial effect of VC on CR-HvKP strains was further tested in a mouse infection model. Mice infected with 1.0×10^4 CFU KP1088 died within 60 hpi when treated with saline alone, but the survival rate increased to 70 and 80% when treated with 20 mg/kg and 80 mg/kg VC, respectively (Figure 8A). The

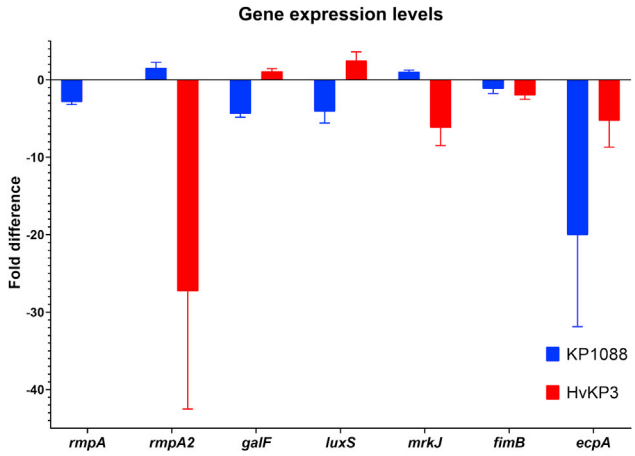

Figure 7. qRT-PCR analysis of CR-hvKP treated with VC

Fold expression of the mucoid phenotype-encoding genes, fimbriae genes, and biofilm-related genes in *K. pneumoniae* strain KP1088 and HvKP3 cells with or without treatment with VC at concentrations of 0.5 × and 0.25 × MIC, respectively. Mean ± SD from three replicates are depicted

therapeutic effect of VC on mice infected with 6.4×10^4 CFU HvKP3 was also tested. Mice treated with saline alone died within 48 hpi, but treatment with 20 mg/kg and 80 mg/kg of VC could lead to 50 and 30% survival of the mice within 72 hpi, respectively (Figure 8B).

The clinical value of VC in treatment of human diseases has been widely discussed but remains controversial (Naidu, 2003). It is well known that VC is both antioxidant (inhibiting oxidation reaction) and prooxidant (inducing oxidative stress), depending on the intracellular and extracellular concentration of VC, as well as the cellular environment (Podmore et al., 1998; Frei et al., 1989). The antibacterial effect of VC *in vitro* was widely described in previous studies. VC is known to exhibit inhibitory effects on bacterial species such as *S. aureus* (Isela et al., 2013), *M. tuberculosis* (Vilchèze et al., 2013), *E. coli* (Shivaprasad et al., 2021), *Helicobacter pylori* (Tabak et al., 2003), *Campylobacter jejuni* (Ghosh et al., 2019), Salmonella *Enteritidis* (Hernandez-Patlan et al., 2018), and fungi such as *Aspergillus niger* and *A. flavus* (Gupta and Guha, 1941) and inhibit biofilm formation by inhibiting EPS production (Pandit et al., 2017; Helgadóttir et al., 2017). The sterilization effect of VC at high concentration was because of the production of ROS through eliciting the Fenton reaction in the presence of Fe^{3+}(Shivaprasad et al., 2021; Vilchèze et al., 2013). The reaction occurs in the presence of metal ions, such as Fe^{3+}, in acidic environment. The acidity of the medium containing high concentration VC created the condition required for onset of the Fenton reaction (Pehlivan, 2017). It should be noted that the Fenton reaction was limited in the human body in which metal-binding proteins could sequestrate free metal ions (e.g. ferric ions) (Carr and Frei, 1999). Previous studies demonstrated that hvKP strains encode ferrichrome, as well as ferric, ferrous and heme iron uptake systems, so that the level of ferric ions is relatively high in hvKP strains (Hsieh et al., 2008; Choby et al., 2020). The chemically diverse siderophores produced by hvKP included aerobactin, yersiniabactin, salmochelin, and enterobactin, the activity of which was reported to be six- to 10-fold higher than that of cKP (Russo et al., 2015). The large amount of ferric ions in bacterial cells renders Fenton reaction possible *in vivo*. In this study, we employed two CR-hvKP strains, KP1088 and HvKP3 to study the antibacterial potential of VC on CR-hvKP; our results showed that VC could eradicate the two strains, with MICs being 8 mg/mL and 16 mg/mL, respectively. The antimicrobial potential of VC on CR-hvKP was higher than that on *E. coli* (MIC at around 22 mg/mL) as reported previously (Shivaprasad et al., 2021). The bactericidal effect of VC on CR-hvKP strains is because of the prooxidant properties of VC. Intracellular VC stimulated the production of excess intracellular ROS, which causes DNA damage, lipid peroxidation, protein denaturation, and finally cell death (Rowe et al., 2008; Khan et al., 2019, Cabiscol et al., 2000).

Formation of biofilm enhances the ability of bacteria to colonize and cause infections in the gastrointestinal, respiratory, and urinary tract by conferring protection against environmental stresses and antimicrobial agents (Piperaki et al., 2017). Reduction in the amount of biofilm renders bacterial cells more exposed to the hazardous environment. EPS is the major component of the biofilm matrix (da Silva et al., 2019). In this

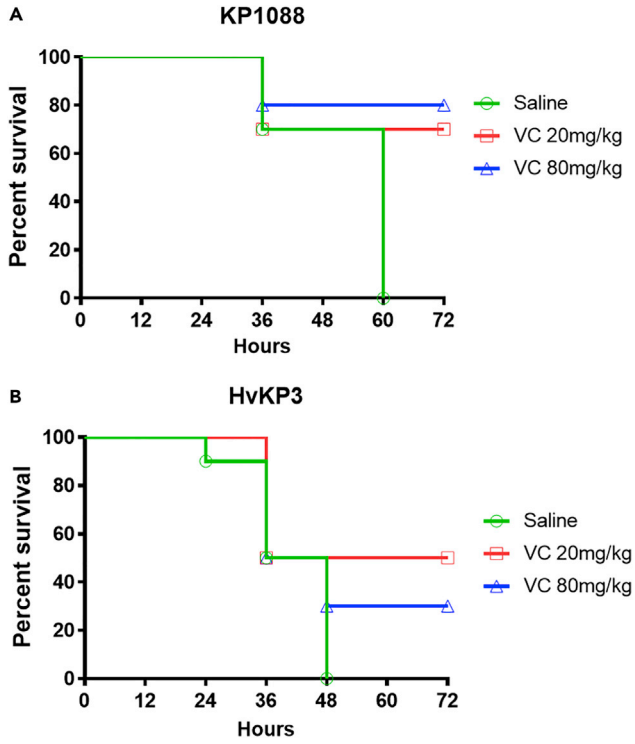

Figure 8. Mouse infection model

(A and B) Efficacy of VC in mouse infection model with strain KP1088 (A) and HvKP3 (B) as infecting agent. Neutropenic NIH mice were infected intraperitoneally with 1.0×10^4 CFU of KP1088 and 6.4×10^4 CFU of HvKP3, respectively, followed by treatment with saline (control), VC at 20 mg/kg and VC at 80 mg/kg. Each mouse was treated five times, with 12 h interval between each treatment. The number of dead mice was recorded at each treatment

study, we found that production of EPS was significantly reduced in the presence of VC at a concentration of 4 mg/mL or higher, thereby effectively inhibiting biofilm formation.

Efflux pumps play an important role in the development and maintenance of biofilms by transporting the required molecules for formation of biofilm; these include EPS and quorum sensing associated molecules (Reza et al., 2019). Results in this study suggest that the activities of efflux pumps were inhibited by VC in a dose-dependent manner, resulting in disruption of EPS transportation and biofilm formation.

CPS and fimbrial adhesins were both major virulence factors in hvKP (Khaertynov et al., 2018). Results in this study showed that production of CPS was suppressed in the presence of 4 mg/mL of VC. As CPS must be exported to the bacterial surface through efflux activities, the inhibition effect of VC on efflux also affects formation of the capsule (Figure 9).

Limitations of the study

In this study, VC at relatively high concentrations (20 and 80 mg/kg) was used to treat infections caused by CR-hvKP and the treatment with 20 mg/kg and 80 mg/kg of VC could lead to 50 and 30% survival of the mice infected with HvKP3 within 72 hpi, respectively (Figure 8B). In a previous study, VC was reported to enhance the treatment efficacy of rifampin on *M. tuberculosis* and the combination of the two drugs could reduce the bacterial burden (Vilchèze et al., 2018). The combinational use of VC and other antibiotics might further enhance the sterilizing effect and shorten infections treatment. Furthermore, the prevention of the formation of persister cells caused by VC was not investigated in this study. These could be potential directions for future study.

CONCLUSIONS

The emergence of CR-hvKP threatens human health as therapeutics options for treatment of infections caused by this pathogen have become extremely limited. There is an urgent need to develop

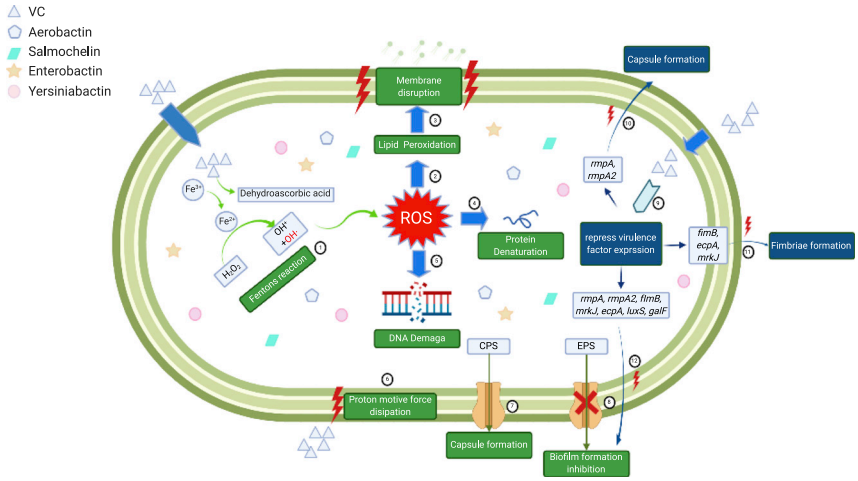

Figure 9. Schematic representation of the antimicrobial and anti-virulence mechanisms of VC

ROS (OH·) was generated in Fenton's reaction induced by intracellular VC①. ROS storm causes damages to bacterial cells including lipid peroxidation②, membrane disruption③, protein denaturation④ and DNA breakage⑤, resulting in collapse of the cell structure. Extracellular VC also causes dissipation in bacterial membrane proton motive force ⑥, which drives efflux activities. As a result, transportation of EPS was hampered ⑦, so that the biofilm formation was inhibited. In addition, export of CPS to the bacterial cell surface was also disrupted when efflux activities were inhibited ⑧. VC also inhibits expression of genes that encode various virulence factors ⑨, including *rmpA* and *rmpA2* (capsule formation) ⑩, *fimB*, *mrkJ*, and *ecpA* (fimbriae formation) ⑪ and *luxS*, *galF*, *fimB*, *mrkJ*, *ecpA*, *rmpA*, *and rmpA2* (biofilm formation) ⑫. Graphical abstract was created with BioRender.com (license number *GP23G531KW*).

antimicrobials which are safe and ready for clinical use. In this study, we not only identified VC as a potential antibacterial agent against CR-hvKP with minimal chance of resistance development, but also validated its bactericidal effect in the mouse infection model. ROS production induced by VC exerts a strong bactericidal effect in a dose-dependent manner. In addition, we found that VC at subminimum inhibitory concentration (sub-MIC) could inhibit the activity of efflux pump, resulting in disruption of EPS transportation and biofilm formation.Furthermore, VC is also an efficient anti-virulence agent which suppresses the production and transportation of CPS, as well as the expression of various virulence-associated genes including *rmpA* and *rmpA2*, *fimB*, *ecpA*, and *mrkJ*. Based on these functional properties, we believe that VC may serve as a reliable antimicrobial agent against CR-hvKP and possibly other bacterial pathogens.

STAR★METHODS

Detailed methods are provided in the online version of this paper and include the following:

- KEY RESOURCES TABLE
- RESOURCE AVAILABILITY
  - Lead contact
  - Materials availability
  - Data and code availability
- EXPERIMENTAL MODEL AND SUBJECT DETAILS
  - Bacterial strains and reagents
  - Strain culturing
  - *In vivo* animal studies
- METHOD DETAILS
  - Antimicrobial susceptibility tests
  - Assessment of anti-biofilm effect
  - Observation of biofilm structure with confocal laser scanning microscopy (CLSM) and scanning electronic microscopy (SEM)
  - Assessment of accumulation of reactive oxygen species (ROS)
  - Extracellular polymeric substance production
  - Quantification of capsule polysaccharide by uronic acid assay
  - Membrane potential assays using 3,3′-Dipropylthiadicarbocyanineiodide [DiSC3(5)]

ACKNOWLEDGMENTS

This research was supported by the Research Impact Fund (R5011-18F) of the Hong Kong Research Grant Council.

AUTHOR CONTRIBUTIONS

C.X. initiated the project, performed the experiments, and drafted the manuscript. N.D. helped with the qPCR analysis. K.C.C. and X.M.Y. performed animal experiments. P.Z. helped with SEM imaging. C.S.H. helped with CLSM imaging. E.W.C.C. helped with experimental design and manuscript writing. X.Y. supervised the project. S.C. designed the experiments, supervised the project, and edited the manuscript.

DECLARATION OF INTERESTS

The authors declare no competing interests.

Received: September 20, 2021
Revised: December 15, 2021
Accepted: February 4, 2022
Published: March 18, 2022

REFERENCES

Alcántar-Curiel, M.D., Blackburn, D., Saldaña, Z., Gayosso-Vázquez, C., Iovine, N.M., De la Cruz, M.A., and Girón, J.A. (2013). Multi-functional analysis of Klebsiella pneumoniae fimbrial types in adherence and biofilm formation. Virulence *4*, 129–138.

Ares, M.A., Fernández-Vázquez, J.L., Rosales-Reyes, R., Jarillo-Quijada, M.D., von Bargen, K., Torres, J., González-y-Merchand, J.A., Alcántar-Curiel, M.D., and De la Cruz, M.A. (2016). H-NS nucleoid protein controls virulence features of Klebsiella pneumoniae by regulating the expression of type 3 pili and the capsule polysaccharide. Front. Cell. Infect. Microbiol. *6*, 13.

Baron, S.A., and Rolain, J.-M. (2018). Efflux pump inhibitor CCCP to rescue colistin susceptibility in mcr-1 plasmid-mediated colistin-resistant strains and gram-negative bacteria. J. Antimicrob. Chemother. *73*, 1862–1871.

Bohnert, J.A., Karamian, B., and Nikaido, H. (2010). Optimized nile red efflux assay of AcrAB-TolC multidrug efflux system shows competition between substrates. Antimicrob. Agents Chemother. *54*, 3770–3775.

Borer, A., Eskira, S., Nativ, R., Saidel-Odes, L., Riesenberg, K., Livshiz-Riven, I., Schlaeffer, F., Sherf, M., and Peled, N. (2011). A multifaceted intervention strategy for eradication of a hospital-wide outbreak caused by carbapenem-resistant Klebsiella pneumoniae in Southern Israel. Infect. Control Hosp. Epidemiol. *32*, 1158–1165.

Cabiscol, E., Tamarit, J., and Ros, J. (2000). Oxidative stress in bacteria and protein damage by reactive oxygen species. Int. Microbiol. *3*, 3–8.

Carr, A., and Frei, B. (1999). Does vitamin C act as a pro-oxidant under physiological conditions? FASEB J. *13*, 1007–1024.

Cescutti, P. (2010). Bacterial capsular polysaccharides and exopolysaccharides. Microb. Glycobiol. *2010*, 93–108.

Chen, Y., and Chen, Y. (2021). Clinical challenges with hypervirulent Klebsiella pneumoniae (hvKP) in China. J. Transl. Intern. Med. *9*, 71–75.

Chhibber, S., Gondil, V.S., Sharma, S., Kumar, M., Wangoo, N., and Sharma, R.K. (2017). A novel approach for combating Klebsiella pneumoniae biofilm using histidine functionalized silver nanoparticles. Front. Microbiol. *8*, 1104.

Choby, J., Howard-Anderson, J., and Weiss, D. (2020). Hypervirulent Klebsiella pneumoniae–clinical and molecular perspectives. J. Intern. Med. *287*, 283–300.

da Silva, D.P., Matwichuk, M.L., Townsend, D.O., Reichhardt, C., Lamba, D., Wozniak, D.J., and Parsek, M.R. (2019). The Pseudomonas aeruginosa lectin LecB binds to the exopolysaccharide Psl and stabilizes the biofilm matrix. Nat. Commun. *10*, 1–11.

Decré, D., Verdet, C., Emirian, A., Le Gourrierec, T., Petit, J.-C., Offenstadt, G., Maury, E., Brisse, S., and Arlet, G. (2011). Emerging severe and fatal infections due to Klebsiella pneumoniae in two university hospitals in France. J. Clin. Microbiol. *49*, 3012–3014.

Dridi, B., Lupien, A., Bergeron, M.G., Leprohon, P., and Ouellette, M. (2015). Differences in antibiotic-induced oxidative stress responses between laboratory and clinical isolates of Streptococcus pneumoniae. Antimicrob. Agents Chemother. *59*, 5420–5426.

Dubois, M., Gilles, K.A., Hamilton, J.K., Rebers, P.T., and Smith, F. (1956). Colorimetric method for determination of sugars and related substances. Anal. Chem. *28*, 350–356.

Extremina, C., Costa, L., Aguiar, A., Peixe, L., and Fonseca, A. (2011). Optimization of processing conditions for the quantification of enterococci biofilms using microtitre-plates. J. Microbiol. Methods *84*, 167–173.

Frei, B., England, L., and Ames, B.N. (1989). Ascorbate is an outstanding antioxidant in human blood plasma. Proc. Natl. Acad. Sci. U S A *86*, 6377–6381.

Furlan, J.P.R., Savazzi, E.A., and Stehling, E.G. (2020). Genomic insights into multidrug-resistant and hypervirulent Klebsiella pneumoniae co-harboring metal resistance genes in aquatic environments. Ecotoxicol. Environ. Saf. *201*, 110782.

Ghosh, T., Srivastava, S.K., Gaurav, A., Kumar, A., Kumar, P., Yadav, A.S., Pathania, R., and Navani, N.K. (2019). A combination of linalool, vitamin C, and copper synergistically triggers reactive oxygen species and DNA damage and inhibits Salmonella enterica subsp. enterica Serovar Typhi and Vibrio fluvialis. Appl. Environ. Microbiol. *85*, e02487–18.

Gomes, A.É.I., Stuchi, L.P., Siqueira, N.M.G., Henrique, J.B., Vicentini, R., Ribeiro, M.L., Darrieux, M., and Ferraz, L.F.C. (2018). Selection and validation of reference genes for gene expression studies in Klebsiella pneumoniae using Reverse Transcription Quantitative real-time PCR. Sci. Rep. *8*, 1–14.

Gu, D., Dong, N., Zheng, Z., Lin, D., Huang, M., Wang, L., Chan, E.W.-C., Shu, L., Yu, J., and Zhang, R. (2018). A fatal outbreak of ST11 carbapenem-resistant hypervirulent Klebsiella pneumoniae in a Chinese hospital: a molecular epidemiological study. Lancet Infect. Dis. *18*, 37–46.

Gupta, G., and Guha, B. (1941). The effect of vitamin C and certain other substances on the growth of microorganisms. Ann. Biochem. Exp. Med. *1*, 14.

Helgadóttir, S., Pandit, S., Mokkapati, V.R., Westerlund, F., Apell, P., and Mijakovic, I. (2017). Vitamin C pretreatment enhances the antibacterial effect of cold atmospheric plasma. Front. Cell Infect. Microbiol. *7*, 43.

Hernandez-Patlan, D., Solis-Cruz, B., Méndez-Albores, A., Latorre, J.D., Hernandez-Velasco, X., Tellez, G., and López-Arellano, R. (2018). Comparison of PrestoBlue® and plating method to evaluate antimicrobial activity of ascorbic acid, boric acid and curcumin in an in vitro gastrointestinal model. J. Appl. Microbiol. *124*, 423–430.

Heydorn, A., Nielsen, A.T., Hentzer, M., Sternberg, C., Givskov, M., Ersbøll, B.K., and Molin, S. (2000). Quantification of biofilm structures by the novel computer program COMSTAT. Microbiology *146*, 2395–2407.

Hodges, R.E., Baker, E.M., Hood, J., Sauberlich, H.E., and March, S.C. (1969). Experimental scurvy in man. Am. J. Clin. Nutr. *22*, 535–548.

Hsieh, P.-F., Lin, T.-L., Lee, C.-Z., Tsai, S.-F., and Wang, J.-T. (2008). Serum-induced iron-acquisition systems and TonB contribute to virulence in Klebsiella pneumoniae causing primary pyogenic liver abscess. J. Infect. Dis. *197*, 1717–1727.

Isela, N.-N.R., Sergio, N.-C., Martínez-Sanmiguel, J.J., Hernandez-Delgadillo, R., and Cabral-Romero, C. (2013). Ascorbic acid on oral microbial growth and biofilm formation. Pharma Innov. *2*, 103.

Jung, J.-H., Choi, N.-Y., and Lee, S.-Y. (2013). Biofilm formation and exopolysaccharide (EPS) production by Cronobacter sakazakii depending on environmental conditions. Food Microbiol. *34*, 70–80.

Kalpoe, J.S., Sonnenberg, E., Factor, S.H., del Rio Martin, J., Schiano, T., Patel, G., and Huprikar, S. (2012). Mortality associated with carbapenem-resistant Klebsiella pneumoniae infections in liver transplant recipients. Liver Transplant. *18*, 468–474.

Karlsson, M., Stanton, R.A., Ansari, U., McAllister, G., Chan, M.Y., Sula, E., Grass, J.E., Duffy, N., Anacker, M.L., Witwer, M.L., et al. (2019). Identification of a carbapenemase-producing hypervirulent Klebsiella pneumoniae isolate in the United States. Antimicrob. Agents Chemother. *63*, e00519–19.

Khaertynov, K.S., Anokhin, V.A., Rizvanov, A.A., Davidyuk, Y.N., Semyenova, D.R., Lubin, S.A., and Skvortsova, N.N. (2018). Virulence factors and antibiotic resistance of Klebsiella pneumoniae strains isolated from neonates with sepsis. Front. Med. *5*, 225.

Khan, S., Rayis, M., Rizvi, A., Alam, M.M., Rizvi, M., and Naseem, I. (2019). ROS mediated antibacterial activity of photoilluminated riboflavin: a photodynamic mechanism against nosocomial infections. Toxicol. Rep. *6*, 136–142.

Knecht, L.E., Veljkovic, M., and Fieseler, L. (2020). Diversity and function of phage encoded depolymerases. Front. Microbiol. *10*, 2949.

Lee, C.R., Lee, J.H., Park, K.S., Jeon, J.H., Kim, Y.B., Cha, C.-J., Jeong, B.C., and Lee, S.H. (2017). Antimicrobial resistance of hypervirulent Klebsiella pneumoniae: epidemiology, hypervirulence-associated determinants, and resistance mechanisms. Front. Cell. Infect. Microbiol. *7*, 483.

Lee, C.-R., Lee, J.H., Park, K.S., Kim, Y.B., Jeong, B.C., and Lee, S.H. (2016). Global dissemination of carbapenemase-producing Klebsiella pneumoniae: epidemiology, genetic context, treatment options, and detection methods. Front. Microbiol. *7*, 895.

Lee, C.-R., Park, K.S., Lee, J.H., Jeon, J.H., Kim, Y.B., Jeong, B.C., and Lee, S.H. (2018). The threat of carbapenem-resistant hypervirulent Klebsiella pneumoniae (CR-HvKP). Biomed. Res. *29*, 2438–2441. https://doi.org/10.4066/biomedicalresearch.66-18-535.

Li, X.-Z., Plésiat, P., and Nikaido, H. (2015). The challenge of efflux-mediated antibiotic resistance in Gram-negative bacteria. Clin. Microbiol. Rev. *28*, 337–418.

Lin, C.T., Wu, C.-C., Chen, Y.S., Lai, Y.-C., Chi, C., Lin, J.-C., Chen, Y., and Peng, H.-L. (2011). Fur regulation of the capsular polysaccharide biosynthesis and iron-acquisition systems in Klebsiella pneumoniae CG43. Microbiology *157*, 419–429.

Lin, T.-H., Wu, C.-C., Kuo, J.-T., Chu, H.-F., Lee, D.-Y., and Lin, C.-T. (2019). FNR-dependent RmpA and RmpA2 regulation of capsule polysaccharide biosynthesis in Klebsiella pneumoniae. Front. Microbiol. *10*, 2436.

Ling, L.L., Schneider, T., Peoples, A.J., Spoering, A.L., Engels, I., Conlon, B.P., Mueller, A., Schäberle, T.F., Hughes, D.E., and Epstein, S. (2015). A new antibiotic kills pathogens without detectable resistance. Nature *517*, 455–459.

Liu, W., Dong, N., and Zhang, X.H. (2012). Overexpression of mltA in Edwardsiella tarda reduces resistance to antibiotics and enhances lethality in zebra fish. J. Appl. Microbiol. *112*, 1075–1085.

Liu, Y., Jia, Y., Yang, K., Li, R., Xiao, X., Zhu, K., and Wang, Z. (2020). Metformin restores tetracyclines susceptibility against multidrug resistant bacteria. Adv. Sci. *7*, 1902227.

Mah, T.F.C., and O'toole, G.A. (2001). Mechanisms of biofilm resistance to antimicrobial agents. Trends Microbiol. *9*, 34–39.

Majkowska-Skrobek, G., Łątka, A., Berisio, R., Maciejewska, B., Squeglia, F., Romano, M., Lavigne, R., Struve, C., and Drulis-Kawa, Z. (2016). Capsule-targeting depolymerase, derived from Klebsiella KP36 phage, as a tool for the development of anti-virulent strategy. Viruses *8*, 324.

Morin, N., Lanneluc, I., Connil, N., Cottenceau, M., Pons, A.M., and Sablé, S. (2011). Mechanism of bactericidal activity of microcin L in Escherichia coli and Salmonella enterica. Antimicrob. Agents Chemother. *55*, 997–1007.

Naidu, K.A. (2003). Vitamin C in human health and disease is still a mystery? An overview. Nutr. J. *2*, 1–10.

Namikawa, H., Oinuma, K.I., Sakiyama, A., Tsubouchi, T., Tahara, Y.O., Yamada, K., Niki, M., Takemoto, Y., Miyata, M., Kaneko, Y., et al. (2019). Discovery of anti-mucoviscous activity of rifampicin and its potential as a candidate antivirulence agent against hypervirulent Klebsiella pneumoniae. Int. J. Antimicrob. Agents *54*, 167–175.

Njus, D., Kelley, P.M., Tu, Y.-J., and Schlegel, H.B. (2020). Ascorbic acid: the chemistry underlying its antioxidant properties. Free Radic. Biol. Med. *159*, 37–43.

Opoku-Temeng, C., Kobayashi, S.D., and Deleo, F.R. (2019). Klebsiella pneumoniae capsule polysaccharide as a target for therapeutics and vaccines. Comput. Struct. Biotechnol. J. *17*, 1360–1366.

Ostapska, H., Howell, P.L., and Sheppard, D.C. (2018). Deacetylated microbial biofilm exopolysaccharides: it pays to be positive. PLoS Pathog. *14*, e1007411.

Paczosa, M.K., and Mecsas, J. (2016). Klebsiella pneumoniae: going on the offense with a strong defense. Microbiol. Mol. Biol. Rev. *80*, 629–661.

Padayatty, S.J., Katz, A., Wang, Y., Eck, P., Kwon, O., Lee, J.-H., Chen, S., Corpe, C., Dutta, A., and Dutta, S.K. (2003). Vitamin C as an antioxidant: evaluation of its role in disease prevention. J. Am. Coll. Nutr. *22*, 18–35.

Pandit, S., Ravikumar, V., Abdel-Haleem, A.M., Derouiche, A., Mokkapati, V., Sihlbom, C., Mineta, K., Gojobori, T., Gao, X., and Westerlund, F. (2017). Low concentrations of vitamin C reduce the synthesis of extracellular polymers and destabilize bacterial biofilms. Front. Microbiol. *8*, 2599.

Pehlivan, F.E. (2017). Vitamin C: An Antioxidant Agent. Vitamin C, pp. 23–35.

Piperaki, E.-T., Syrogiannopoulos, G.A., Tzouvelekis, L.S., and Daikos, G.L. (2017). Klebsiella pneumoniae: virulence, biofilm and antimicrobial resistance. Pediatr. Infect. Dis. J. *36*, 1002–1005.

Podmore, I.D., Griffiths, H.R., Herbert, K.E., Mistry, N., Mistry, P., and Lunec, J. (1998). Vitamin C exhibits pro-oxidant properties. Nature *392*, 559.

Qian, W., Wang, W., Zhang, J., Wang, T., Liu, M., Yang, M., Sun, Z., Li, X., and Li, Y. (2020). Antimicrobial and antibiofilm activities of ursolic acid against carbapenem-resistant Klebsiella pneumoniae. J. Antibiot. *73*, 382–391.

Reens, A.L., Crooks, A.L., Su, C.-C., Nagy, T.A., Reens, D.L., Podoll, J.D., Edwards, M.E., Yu, E.W., and Detweiler, C.S. (2018). A cell-based infection assay identifies efflux pump modulators that reduce bacterial intracellular load. PLoS Pathog. *14*, e1007115.

Reza, A., Sutton, J.M., and Rahman, K.M. (2019). Effectiveness of efflux pump inhibitors as biofilm disruptors and resistance breakers in gram-negative (ESKAPEE) bacteria. Antibiotics *8*, 229.

Ribeiro, S.M., Cardoso, M.H., Candido, E.D.S., and Franco, O.L. (2016). Understanding, preventing and eradicating Klebsiella pneumoniae biofilms. Future Microbiol. *11*, 527–538.

Rinaudo, C.D., Rosini, R., Galeotti, C.L., Berti, F., Necchi, F., Reguzzi, V., Ghezzo, C., Telford, J.L., Grandi, G., and Maione, D. (2010). Specific involvement of pilus type 2a in biofilm formation in group B Streptococcus. PLoS One *5*, e9216.

Rowe, L.A., Degtyareva, N., and Doetsch, P.W. (2008). DNA damage-induced reactive oxygen species (ROS) stress response in Saccharomyces cerevisiae. Free Radic. Biol. Med. *45*, 1167–1177.

Russo, T.A., Olson, R., Macdonald, U., Beanan, J., and Davidson, B.A. (2015). Aerobactin, but not yersiniabactin, salmochelin, or enterobactin, enables the growth/survival of hypervirulent (hypermucoviscous) Klebsiella pneumoniae ex vivo and in vivo. Infect. Immun. *83*, 3325–3333.

Schmid, J., Sieber, V., and Rehm, B. (2015). Bacterial exopolysaccharides: biosynthesis pathways and engineering strategies. Front. Microbiol. *6*, 496.

Sellick, J.A., and Russo, T.A. (2018). Getting hypervirulent Klebsiella pneumoniae on the radar screen. Curr. Opin. Infect. Dis. *31*, 341–346.

Shivaprasad, D., Taneja, N.K., Lakra, A., and Sachdev, D. (2021). In vitro and in situ abrogation of biofilm formation in E. coli by vitamin C through ROS generation, disruption of quorum sensing and exopolysaccharide production. Food Chem. *341*, 128171.

Shon, A.S., Bajwa, R.P., and Russo, T.A. (2013). Hypervirulent (hypermucoviscous) Klebsiella pneumoniae: a new and dangerous breed. Virulence *4*, 107–118.

Tabak, M., Armon, R., Rosenblat, G., Stermer, E., and Neeman, I. (2003). Diverse effects of ascorbic acid and palmitoyl ascorbate on Helicobacter pylori survival and growth. FEMS Microbiol. Lett. *224*, 247–253.

Te Winkel, J.D., Gray, D.A., Seistrup, K.H., Hamoen, L.W., and Strahl, H. (2016). Analysis of antimicrobial-triggered membrane depolarization using voltage sensitive dyes. Front. Cell Dev. Biol. *4*, 29.

Turton, J.F., Englender, H., Gabriel, S.N., Turton, S.E., Kaufmann, M.E., and Pitt, T.L. (2007). Genetically similar isolates of Klebsiella pneumoniae serotype K1 causing liver abscesses in three continents. J. Med. Microbiol. *56*, 593–597.

Victor, L.Y., Hansen, D.S., Ko, W.C., Sagnimeni, A., Klugman, K.P., Von Gottberg, A., Goossens, H., Wagener, M.M., Benedi, V.J., and Group, I.K.S. (2007). Virulence characteristics of Klebsiella and clinical manifestations of K. pneumoniae bloodstream infections. Emerg. Infect. Dis. *13*, 986.

Vilchèze, C., Hartman, T., Weinrick, B., and Jacobs, W.R. (2013). Mycobacterium tuberculosis is extraordinarily sensitive to killing by a vitamin C-induced Fenton reaction. Nat. Commun. *4*, 1–10.

Vilchèze, C., Kim, J., and Jacobs, W.R., JR. (2018). Vitamin C potentiates the killing of Mycobacterium tuberculosis by the first-line tuberculosis drugs isoniazid and rifampin in mice. Antimicrob. Agents Chemother. *62*, e02165–17.

Vorregaard, M. (2008). Comstat2-a Modern 3D Image Analysis Environment for Biofilms (Citeseer), pp. 1–85.

Vu, B., Chen, M., Crawford, R.J., and Ivanova, E.P. (2009). Bacterial extracellular polysaccharides involved in biofilm formation. Molecules *14*, 2535–2554.

Walker, K.A., Miner, T.A., Palacios, M., Trzilova, D., Frederick, D.R., Broberg, C.A., Sepúlveda, V.E., Quinn, J.D., and Miller, V.L. (2019). A Klebsiella pneumoniae regulatory mutant has reduced capsule expression but retains hypermucoviscosity. mBio *10*, e00089–19.

Xu, C., Chen, K., Chan, K.F., Chan, E.W.C., Guo, X., Chow, H.Y., Zhao, G., Zeng, P., Wang, M., and Zhu, Y. (2020). Imidazole type Antifungal drugs are effective colistin adjuvants that resensitize colistin-resistant enterobacteriaceae. Adv. Ther. *3*, 2000084.

Zhang, R., Lin, D., Chan, E.W.C., Gu, D., Chen, G.X., and Chen, S. (2016a). Emergence of carbapenem-resistant serotype K1 hypervirulent Klebsiella pneumoniae strains in China. Antimicrob. Agents Chemother. *60*, 709–711.

Zhang, Y., Zhao, C., Wang, Q., Wang, X., Chen, H., Li, H., Zhang, F., Li, S., Wang, R., and Wang, H. (2016b). High prevalence of hypervirulent Klebsiella pneumoniae infection in China: geographic distribution, clinical characteristics, and antimicrobial resistance. Antimicrob. Agents Chemother. *60*, 6115–6120.

Zhao, Y., Zhang, X., Torres, V.V.L., Liu, H., Rocker, A., Zhang, Y., Wang, J., Chen, L., Bi, W., and Lin, J. (2019). An outbreak of carbapenem-resistant and hypervirulent Klebsiella pneumoniae in an intensive care unit of a major teaching hospital in Wenzhou, China. Front. Public Health *7*, 229.

STAR★METHODS

KEY RESOURCES TABLE

REAGENT or RESOURCE	SOURCE	IDENTIFIER
Bacterial strains		
KP1088	Patients in our previous studies (Zhang et al., 2016b)	N/A
HvKP3	Patients in our previous studies (Gu et al., 2018)	N/A
Chemicals, peptides, and recombinant proteins		
Vitamin C (ascorbic acid)	Sigma-Aldrich	CAS: 50-81-7
Critical commercial assays		
SYTOX™ Green Nucleic Acid Stain	ThermoFisher	Catalog number: S7020
DiSC3(5) (3,3′-Dipropylthiadicarbocyanine Iodide) Stain	ThermoFisher	Catalog number: D306
CM-H2DCFDA (General Oxidative Stress Indicator)	ThermoFisher	Catalog number: C6827
Software and algorithms		
Graphpad Prism 8	GraphPad Software Inc. San Diego, CA, USA	https://www.graphpad.com/
COMSTAT	Technical University of Denmark, Lyngby, Denmark	http://www.comstat.dk/

RESOURCE AVAILABILITY

Lead contact

Further information and requests for resources and reagents should be directed to and will be fulfilled by the lead contact Sheng CHEN (shechen@cityu.edu.hk).

Materials availability

This study did not generate new unique reagent

Data and code availability

All data used in this manuscript are time-kill curves, microscopy images. All data are available upon request from the corresponding author. This paper does not report original code. Any additional information required to reanalyze the data reported in this paper is available from the lead contact upon request.

EXPERIMENTAL MODEL AND SUBJECT DETAILS

Bacterial strains and reagents

CR-hvKP strains HvKP3 and KP1088 were isolated from patients in our previous studies (Gu et al., 2018; Zhang et al., 2016a). Briefly, *K. pneumoniae* strain KP1088, which belongs to ST11 and serotype K1, was isolated from a 67-year-old patient after surgical treatment of multiple injuries. Strain KP1088 was resistant to carbapenems, cephalosporins, aminoglycosides but susceptible to polymyxins, tigecycline, and quinolones (Zhang et al., 2016a). *K. pneumoniae* strain HvKP3 was isolated from a 65-year-old patient admitted to the hospital after a car accident. Belonging to ST11 and serotype K47, strain HvKP3 was resistant to carbapenems, cephalosporins, monobactams, penicillin, aminoglycoside, quinolones and polymyxins but remained susceptible to tigecycline (Gu et al., 2018). The hypervirulence phenotypes of both strains have been validated by experiments using different animal models previously (Gu et al., 2018; Zhang et al., 2016a). VC, also called L-Ascorbic acid, was purchased from Sigma (USA)

Strain culturing

The strains were grown overnight on LB agar plates or in LB broth with shaking at 250 rpm at 37°C.

In vivo animal studies

Mice were male ICR mice at 4 to 5 weeks. Animal infection experiments were approved by the Research Animal Care and Use Committee of City University of Hong Kong.

METHOD DETAILS

Antimicrobial susceptibility tests

Minimum inhibitory concentration (MIC) of VC on CR-hvKP strains was conducted by using a broth dilution method as described previously and interpreted according to the Clinical & Laboratory Standards Institute guideline. To further determine the bactericidal effect VC on hypervirulent *K. pneumoniae* strain HvKP3 and KP1088, the time-dependent killing curve was determined as described previously with slight modifications (Liu et al., 2020). Briefly, the two strains in the early exponential phase and late exponential phase were treated with a series of concentrations of VC and incubated at 37°C overnight. At each time point, 100μL aliquots were collected and serially diluted for viable counting. The colony counts were conducted in triplicate.

Assessment of anti-biofilm effect

The anti-biofilm effect of VC was evaluated according to methods described previously, with minor modifications (Liu et al., 2012). Briefly, overnight cultures of OD_{600} of 0.1 were incubated with different concentrations of VC for 24 hours without shaking. Sterile TSB medium containing 1% glucose was used as negative control. Cells that were adherent to the wells were stained with 200 μL of 0.1% of crystal violet for 30 minutes. The absorbance of each well was recorded at 540 nm using SpectraMax® ABS Microplate Reader (Molecular Devices, United States). The ability of the test organisms to form biofilm in the presence and absence of VC was evaluated as described previously (Extremina et al., 2011). The average OD values of all test strains and negative controls (nc) was determined and the cut-off value (OD_c) was calculated as the sum of the average OD of the negative control (OD_{NC}) and three standard deviation of negative control (SD_{nc}) [ODc = average ODnc + (3×SDnc)]. The ability of strains to develop biofilms were divided into the following categories:

$OD \leq ODc$ = non biofilm producer;

$ODc < OD \leq 2 \times ODc$ = weak biofilm producer;

$2 \times ODc < OD \leq 4 \times ODc$ = moderate biofilm producer;

$4 \times ODc < OD$ = strong biofilm producer.

Observation of biofilm structure with confocal laser scanning microscopy (CLSM) and scanning electronic microscopy (SEM)

The impact of VC on bacterial biofilm formation was visualized by CLSM according to methods described previously, with slight modifications (Rinaudo et al., 2010). Overnight cultures were inoculated onto a glass slide placed in a Petri dish, and incubated in the presence and absence of VC at 37°C for 24 hours. Cells that adhered to the glass slide were washed and fixed, followed by staining with SYTOX Green. The biofilm was imaged by the Zeiss LSM 880 Confocal Microscope (Jena, Thuringia, Germany) at 488 nm. To further examine the effect of VC on biofilm formation, SEM was performed according to the procedure previously described, with slight modifications (Chhibber et al., 2017). Briefly, biofilm was grown on a sterile glass slide placed in Petri dish and treated with VC as described above. Adherent cells were washed and fixed with 2.5% glutaraldehyde, followed by dehydration with 50% ethanol and 100% ethanol. The biofilm structure was observed using a scanning electron microscope (Tescan VEGA3).

Assessment of accumulation of reactive oxygen species (ROS)

To determine the level of ROS accumulation in strain KP1088 and HvKP3 upon treatment with different concentrations of VC, a DCF-DA assay was performed according to the methods described previously, with slight modifications (Dridi et al., 2015). Briefly, overnight cultures of strain KP1088 and HvKP3 were diluted 100-fold and incubated at 37°C for two hours. The cultures were diluted to an OD_{600} of 0.1 with fresh LB media and treated with different concentrations of VC for 4 hours. The cells were then stained with DCF-DA, followed by measurement of fluorescence using a SpectraMax® iD3 Multi-Mode Microplate Reader (Molecular Devices, Austria).

Extracellular polymeric substance production

Overnight culture of KP1088 and HvKP3 were diluted 100-fold in LB broth and incubated at 37°C for 2 hours. Six mL of the diluted cultures ($1*10^6$ cells/mL) were treated with different concentrations of VC for 12 hours.

Extracellular polymeric substance (EPS) produced by the two test strains were extracted for quantification using the phenol-sulfuric acid assay according to methods described previously (Jung et al., 2013; Dubois et al., 1956).

Quantification of capsule polysaccharide by uronic acid assay

Capsule polysaccharide (CPS) was extracted as described by Domenico *et al* (Walker et al., 2019), with slight modifications. Overnight cultures were diluted 100-fold in 3ml of LB media and incubated at 37°C for 2 hours. Thereafter, the cultures were treated with different concentrations of VC and incubated overnight at 37 °C. The amount of CPS in the treated samples were quantified and expressed in nanograms per 10^6CFU.

Membrane potential assays using 3,3′-Dipropylthiadicarbocyanineiodide [DiSC3(5)]

Bacterial membrane potential was determined using the voltage-sensitive dye [DiSC3(5)] as described previously (Xu et al., 2020). The stained cells were treated with different concentrations of VC, followed by measurement of fluorescence over a 30-minute period by using a SpectraMax® iD3 Multi-Mode Microplate Reader. 5μM of valinomycin was added as the positive control.

Assessment of efflux inhibitory activity of VC

The inhibitory effect of VC on efflux activities was evaluated by using the dye Nile Red according to a method described previously, with some modifications (Reens et al., 2018). Briefly, VC treated bacterial cells (OD_{600} at 1.0) were stained with 5μM of Nile red for 3 hours at 37°C. The sample was then washed and resuspended with Phosphate buffered saline (PBS) containing 1mM $MgCl_2$ and indicated concentraions of VC. In washout experiments, the stained cells were washed and resuspended in PBS with 1mM $MgCl_2$ but not VC. After washing and adding the cells to 96-well black walled plates (~15 minutes), the fluorescence of the cell suspension was monitored for another 2.8 min, after which the cell suspension was triggered with 50 mM of glucose. The fluorescence level was then monitered for another 20 minutes.

Resistance development

The potential of the test strains to develop phenotypic resistance to VC was determined as decribed previously (Xu et al., 2020). Briefly, overnight cultures of the two strains were dilued 100-fold in fresh LB broth containing VC at concentrations of 0.25*MIC, 0.5*MIC, 1*MIC, 2*MIC and 4*MIC, followed by incubation for 24 hours at 37°C. Cultures treated with the second highest concentraions that allowed growth (OD $\geq$ 2) were resuspended in new fresh LB broth containing VC at concentrations of 0.25*MIC, 0.5*MIC, 1*MIC, 2*MIC and diluted100-fold. The serial passage was repeated daily for seven days, recording VC concentrations that supported growth at each passage.

qRT-PCR assays

Total RNA of the test strains was extracted using the QIAGEN RNeasy Mini Kit (Qiagen Inc., Valencia, CA, USA), following the manufacturer's instructions. Extracted RNA was treated with the Invitrogen TURBO DNA-free Kit (Ambion, Austin, TX, USA), followed by reverse transcription using the Invitrogen SuperScript™ III Reverse Transcriptase (Invitrogen, Carlsbad, CA, USA). Quantitative real-time PCR (qRT-PCR) of the target genes was conducted in a Roche LightCycler 480 (Roche Diagnostic Ltd., Basel, Switzerland), using primers reported previously (Lin et al., 2011; Qian et al., 2020; Ares et al., 2016). The *proC* gene of *K. pneumoniae* was amplified with previously published primers and used as an endogenous reference gene (Gomes et al., 2018).

Mouse-infection model

The antimicrobial effect of VC on CR-HvKP strains was tested in an immunocompetent bacteremia infection model according to the method described previously, with some modifications (Xu et al., 2020). In this experiment, male ICR mice were divided into three groups (four mice per group) and infected intraperitoneally with 6.4×10^4 CFU of HvKP3 and 1.0×10^4 CFU of KP1088. At 1 hour post infection (hpi), the mice were injected intraperitoneally with VC at 20 mg/kg and 80 mg/kg, respectively. Four untreated animals were included as control. The mice were treated five times, each separated by 12 h. All animal experiments were approved by the Animal Subjects Ethics Sub-Committee of City University of Hong Kong.

QUANTIFICATION AND STATISTICAL ANALYSIS

All experiments were perfomed in triplicate and all data were presented as means ± SD. Unpaired *t*-test between two groups, or one-way ANOVA, was performed. Graphpad Prism 8 (GraphPad Software Inc. San Diego, CA, USA) was used to calculate the p values (*, $p < 0.05$, **, $p < 0.005$, ***$p < 0.0005$, ****$p < 0.00005$).